The American Mineralogist, Volume 60, pages 898–906, 1975

The Structure of Pseudorutile and Its Role in The Natural Alteration of Ilmenite

IAN E. GREY AND ALAN F. REID

CSIRO, Division of Mineral Chemistry, P.O. Box 124, Port Melbourne, Victoria 3207, Australia

Abstract

Samples of pseudorutile from South Australian and Indonesian localities have been analyzed chemically and studied by X-ray diffraction techniques. A complete structure analysis has been carried out on a single crystal of the Indonesian material. The structure is based on hexagonal close-packed oxygens with metal atoms randomized with two thirds occupancy over half the available octahedral sites and fully ordered in the remaining sites. The ordered atoms form chains of alternately filled and empty octahedral sites along [001]. Poor correlation between these ordered chains leads to diffuse streaking of the metal-ordering reflections in certain planes perpendicular to [001]. We have obtained a satisfactory refinement of the single crystal intensity data for an *average* metal-ordering model defined by a hexagonal cell with $a = 14.375$ Å and $c = 4.615$ Å.

The structural relationships between ilmenite, pseudorutile, and rutile are discussed. A two-stage mechanism for the natural alteration of ilmenite to pseudorutile to rutile is proposed. An electrochemical corrosion model in the zone of saturation is suggested for the initial alteration of ilmenite to pseudorutile. Further alteration to rutile is considered to take place in a zone of oxidation via a dissolution and reprecipitation process.

Introduction

Natural weathering of ilmenite, $FeTiO_3$, involves oxidation of the ferrous iron to ferric, and progressive removal of iron by leaching, resulting eventually in the production of rutile, TiO_2. As early as 1909 (Palmer, 1909) it was recognized that the alteration of ilmenite to rutile proceeded through a distinct intermediate species with approximate composition $Fe_2O_3 \cdot 3TiO_2$. The intermediate alteration phase was termed arizonite by Palmer (1909). Whether arizonite is an independent mineral with a definite structure and composition has been the subject of considerable debate (Miller, 1945; Lynd, Sigurdson, North, and Anderson, 1954; Dyadchenko and Khatuntseva, 1960; Bykov, 1964); a number of researchers supported the alternative thesis that arizonite was a polymineralic mixture of rutile, anatase, hematite, and ilmenite (Ernst, 1943; Overholt, Vaux, and Rodda, 1950). However, regardless of whether it was called arizonite, proarizonite (Bykov, 1964), or amorphous iron-titanate (Bailey, Cameron, Spedden, and Weege, 1956), most researchers were agreed that the alteration of ilmenite proceeded through a distinct intermediate isotropic material with a narrow range of composition, *e.g.* $Fe_2O_3 \cdot nTiO_2 \cdot mH_2O$; $3 < n < 5$ and $1 < m < 2$ (Dyadchenko and Khatuntseva, 1960). Much of the confusion regarding this intermediate alteration compound resulted because the usual method of characterization, powder X-ray diffraction, proved unsatisfactory because of the poor crystallinity of the alteration phases and because of the coincidence of many of the diffraction lines from different phases. These problems were overcome by Teufer and Temple (1966) by the application of single crystal X-ray diffraction techniques to single crystal grains of altered ilmenite from commercial ilmenite concentrates. They identified a new compound with hexagonal symmetry and with composition approximating $Fe_2Ti_3O_9$ as the main constituent of the altered product. Small amounts of auxiliary ilmenite and rutile gave separate, easily identifiable single crystal X-ray patterns. Structure factor calculations were carried out for the new compound, which these authors named pseudorutile. The general structure was shown to consist of a hexagonal close-packed oxygen lattice with metal atoms statistically distributed over the available octahedral sites. However, such a *disordered* model for pseudorutile, with a random distribution of metal atoms, does not readily explain the

consistent composition $Fe_2Ti_3O_9$ closely approximated in occurrences of the mineral as widespread as the U.S.A., India, Russia, Brazil, Indonesia, and Australia. Moreover, the small hexagonal unit cell chosen by Teufer and Temple for random metal atom occupancy, with $a = 2.872$ Å and $c = 4.594$ Å, failed to index a number of the strong diffuse reflections which they observed in the single crystal diffraction patterns.

In the present work we have carried out a single crystal X-ray structure analysis of pseudorutile and have determined the local metal ordering, which appears to contribute to the stability of the $Fe_2Ti_3O_9$ composition. This has enabled us to establish the structural relationships between ilmenite, pseudorutile, and rutile, and to propose a model for the mechanism of alteration of ilmenite.

Present Work

Description of Samples

Samples of carefully purified pseudorutile from Indonesian and South Australian localities were kindly supplied by the Australian Mineral Development Laboratories (Amdel). The occurrence and physical properties of the South Australian sample have previously been described by Larrett and Spencer (1971). A representative set of analyses is reproduced in Table 1. The Indonesian pseudorutile occurs as a major constituent in certain commercial "ilmenite" concentrates produced as by-products of tin processing operations. It has the appearance of a typical beach-sand ilmenite, with grain size mainly in the range 50-200 μm. Indonesian pseudorutile samples were prepared by Amdel by initial density separation in the range 4.0-4.3, followed by magnetic separation. Chemical analyses for the Indonesian pseudorutile (Table 1) show that it contains about five times the manganese content and three times the ferrous iron content of the South Australian material. On the basis of nine oxygen atoms, the calculated formulae are:

South Aust. pseudorutile:

$$Fe^{3+}_{1.81}\,Fe^{2+}_{0.07}\,Mn^{3+}_{0.03}\,Ti^{4+}_{3.08}\,O_9 \cdot 0.75\,H_2O \equiv M_{4.99}O_9 \cdot 3/4\,H_2O$$

Indonesian pseudorutile:

$$Fe^{3+}_{1.34}\,Fe^{2+}_{0.26}\,Mn^{3+}_{0.15}\,Ti^{4+}_{3.25}\,O_9 \cdot 0.48\,H_2O \equiv M_{5.00}O_9 \cdot 1/2\,H_2O$$

i.e., both formulae are close to the ideal M_5O_9 formula, although we have not considered the possibility of some hydroxyl ions in the close packed anion framework.

TABLE 1. Analyses of Materials

Chemical analyses (wt %)	South Australian pseudorutile (Larrett & Spencer, 1971)	South Australian pseudorutile This Work	Indonesian pseudorutile Sample AK.4	Indonesian pseudorutile Sample TP.9	Western Australian altered ilmenite
TiO_2	62.05	58.84	64.01	63.02	59.0
Fe_2O_3	34.20	34.65	24.37	26.00	20.0
FeO	1.50	1.24	4.18	4.51	15.7
Mn_2O_3	0.54	0.60	2.36	2.87	1.4
H_2O, OH^- *	-	3.24	2.56	2.08	0.67
TOTAL	98.29	98.57	97.48	98.48	96.8

**From weight loss on heating to 800°C in air, corrected for oxidation of iron.*

Powder X-ray diffraction patterns for the two pseudorutiles (Fig. 1, iii, iv) show the South Australian sample to be very clean, with lines from other phases completely absent, whereas the Indonesian sample shows extra weak diffraction lines from both rutile and ilmenite.

Also shown in Figure 1 is the diffraction pattern for an altered ilmenite from Western Australia (top, i). This pattern is reproduced closely by the pattern for a mechanical mixture comprising 40 wt percent synthetic ilmenite, 55 wt percent pseudorutile and 5 wt percent rutile (Fig. 1, ii). It is easy to see how the presence of amounts even as large as 50 wt percent of pseudorutile were not detected in early diffraction studies on altered ilmenites. There is almost complete coincidence of the sharp pseudorutile reflections with rutile reflections, and the broad metal-ordering reflections lie underneath strong ilmenite reflections.

Single Crystal X-ray Studies

A number of single crystal grains of both pseudorutiles were studied by X-ray diffraction using both oscillation-Weissenberg and precession methods. Our observations agree with those of Teufer and Temple (1966), *i.e.*, the diffraction patterns showed both sharp, well defined spots and diffuse streaks, or arcs, of considerable intensity. The sharp reflections, indexed by a simple hexagonal cell—$a = 2.875$ Å, $c = 4.615$ Å—represent diffraction from close-packed anion planes and for convenience will be called the fundamental reflections. The diffuse reflections, which were confined to reciprocal layers of the fundamental cell with l odd (Fig. 2), were considered to result from diffraction by a (poorly)

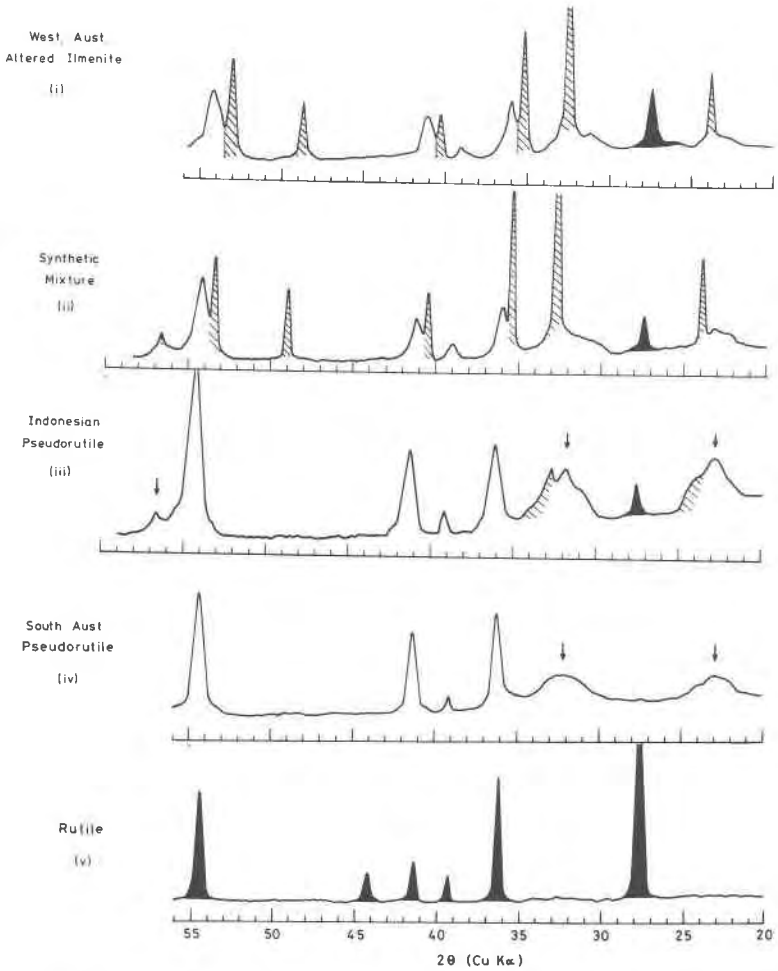

FIG. 1. X-ray powder diffraction patterns. In (i)-(iii), cross-hatching = ilmenite; black shading = rutile; and no shading = pseudorutile peaks. The pattern in (ii) corresponds to a mechanical mixture containing 40 wt percent synthetic ilmenite, 55 wt percent pseudorutile (South Australian sample), and 5 wt percent synthetic rutile. In (iii) and (iv) the metal-ordering peaks are indicated by arrows.

ordered array of the metal atoms. These metal-ordering reflections appear as broad humps (marked with arrows) in the powder patterns shown in Figure 1. For the South Australian pseudorutile, these metal-ordering reflections were so diffuse and elongated that an accurate determination of their positions was very difficult. However, for the Indonesian samples the diffuse reflections were easily resolvable into separate discrete spots with a sharpness approaching that of the fundamental reflections. We were thus able to index the reflections and establish the superlattice defining the metal atom ordering. Consequently, a complete structural analysis was carried out on a single crystal of Indonesian pseudorutile.

Determination of Unit Cell and Space Group

Weissenberg photographs taken with the hexagonal c axis as the oscillation axis showed metal-ordering superstructure reflections only on reciprocal layers with $l = 2n + 1$. If the metal ordering is defined by a superlattice of the fundamental cell in the a-b plane, the indices may be expressed in terms of the fundamental cell indices hkl as $(h/\delta) \pm n$, $(k/\delta) \pm n$, l with n integral and $\delta = 1/m$ where m, integral, represents the superlattice multiplicity, *e.g.* $\delta = 0.25$ corresponds to a $4\times$ superlattice along a and b. From careful measurement of the spot positions on both Weissenberg and precession photographs, it was found that δ was not constant but varied between reflections in the range 0.185-0.195. The averaged

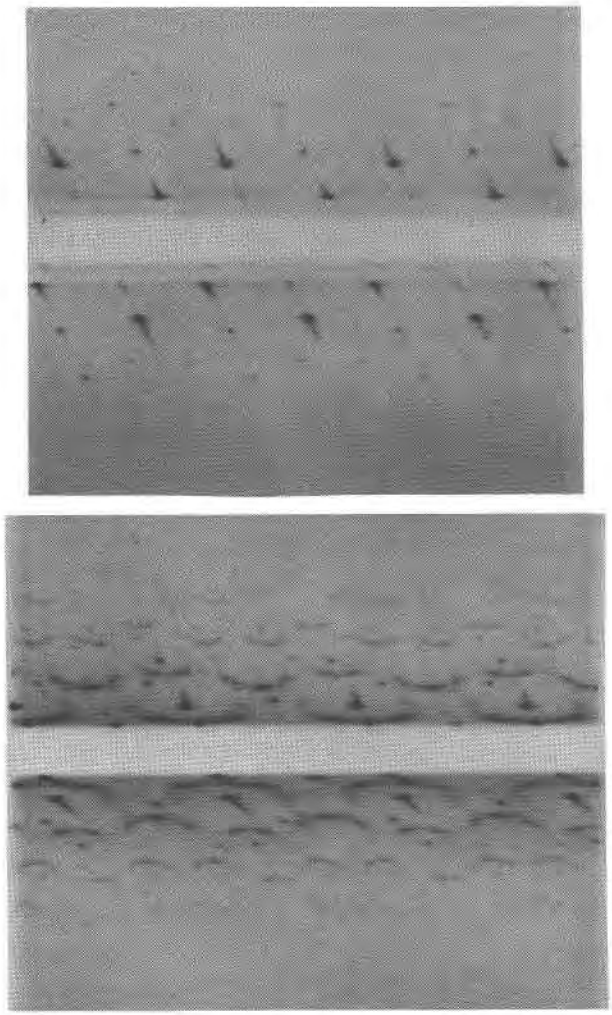

FIG. 2. Reciprocal lattice sections for pseudorutile: *hk*0 (upper), *hk*1 (lower).

value of δ, 0.190, corresponds to a non-integral value of m, the superlattice multiplicity, of 5.26.

A similar situation has been reported by Koch and Cohen (1969) in their structural study on wüstite, $Fe_{1-x}O$, which has a cubic fundamental cell and exhibits superlattice reflections with $\delta = 0.384$, corresponding to $m = 2.60$. This was interpreted to mean that the unit cell defining the superstructure is an integral multiple of the fundamental cell which varies from place to place in the specimen, so that the observed spacing corresponds to the average, non-integral repeat distance. By approximating δ to 0.333, Koch and Cohen derived a satisfactory model for the short range order in terms of a 3× superstructure.

Following this procedure, we approximated δ to 0.200, giving a 5× supercell for pseudorutile of composition $Fe_{1.60}Mn_{0.15}Ti_{3.25}O_{9.00}$—formula weight, 397.3 (Indonesian sample TP-9)—with $a = 14.375(6)$Å and $c = 4.615(3)$Å, $V = 825.9$Å^3. Indices for reflections based on this cell showed only one systematic extinction, $00l$ for $l = 2n + 1$. Hexagonal space groups compatible with this requirement are $P6_3$, $P6_3/m$, and $P6_322$. Of these only the last has the experimentally observed Laue-group symmetry ($6mmm$), and so the space group is unambiguously $P6_322$.

Data Collection

For the collection of intensity data a single crystal of the Indonesian pseudorutile, in the form of a small hexagonal prism, was aligned about the c axis. The crystal measured 0.15 mm along its hexagonal edge and was 0.07 mm thick. Intensity data for the levels *hk*0 to *hk*4 were obtained by the integrated Weissenberg technique, using zirconium-filtered molybdenum radiation. The intensities were estimated visually using a calibrated film strip. The areal dimensions of each of the integrated reflections were carefully measured with a micrometer to correct for the greater spread of the metal-ordering reflections. Lorentz and polarization corrections were applied, but an absorption correction was not considered necessary because of the small crystal size and the low linear absorption (Mo$K\alpha$ radiation) coefficient, 85.7 cm^{-1}.

In the structure factor calculations the iron and titanium atoms were not distinguished, and a composite scattering curve was used, $f(M) = 1/5[2f(Fe^{3+}) + 3f(Ti^{4+})]$. Scattering curves for metals and oxygen, O^{2-}, were taken from *International Tables for X-ray Crystallography* (1962, pp. 201 *ff*). All computing was performed on the Monash University CDC 3200 and the CSIRO CDC 7600 computers. For the least-squares refinement a modified version of the full matrix least-squares program of Busing, Martin, and Levy (1962) was used.

Structure Solution and Refinement

As a basis for our structural models we considered the model proposed by Teufer and Temple (1966), *i.e.*, an hexagonal close-packed oxygen lattice with metal atoms statistically distributed over the octahedral sites. Teufer and Temple reported an R factor of 0.045 for their refinement of this model, using fundamental reflections only. Accordingly, oxygens were arranged in hexagonal close-packed layers at $z = 1/4$ and 3/4, and metals were placed in all the available octahedral sites. This was accomplished in the space group $P6_322$ by placing one atom at the

origin, four atoms in positions 6*g* (x,0,0, *etc.* with x = 1/5, 2/5, 3/5, and 4/5) and two atoms in the general positions 12*i* with x_1, y_1, z_1, = 1/5, 2/5, 0 and x_2, y_2, z_2 = 1/5, 3/5, 0. The equipoints of space group $P6_322$ generate nickel-arsenide-like strings from the metals placed in positions 2*a* and 12*i*, for which M–M = $\frac{1}{2}c$ = 2.30 Å. To prevent this unlikely structural situation, we constrained the site occupancies of these sites to be less than 0.67. The occupancies of the metal atom sites were also constrained to be consistent with the overall stoichiometry of M_6O_9. With these limitations only a few models for the metal atom ordering remained to be considered, and a model was quickly developed which gave good agreement between the observed and calculated structure factors (R = 0.19). It contained two filled 6*g* sites and two empty 6*g* sites and had the 2*a* and 12*i* sites two-thirds filled. The initial ideal model coordinates and site occupancies are given in Table 2.

Following the procedure used by Koch and Cohen (1969) for a similar superstructure problem with limited data, we first refined the scale factors and overall temperature factors for the metals and oxygens, using the fundamental reflections only. These parameters were then fixed and all positional parameters refined, using all observed reflections. In some cases, atom positions for different atoms had to be refined individually because of strong correlation effects. After all atom coordinates had refined satisfactorily, the occupation factors for each of the metal atom sites were refined. A final R factor of 0.069 for all observed data was obtained.

The final positional and occupancy factors, with standard deviations, are listed in Table 2. Table 3 gives the final observed and calculated structure factors.

Discussion

An (001) section of the pseudorutile structure (Fig. 3) shows one hexagonal close-packed oxygen layer. The structure contains metal atom sites exhibiting two types of occupancy, namely one set ordered and one set disordered along *c*. These sites are shown separately by filled and empty circles in Figure 3. The disordered metals statistically occupy two-thirds of the $M(1)$, $M(6)$, and $M(7)$ octahedral sites available to them. The clusters of disordered sites thus resemble segments of ilmenite in which the pairs of octahedral face-shared metals have been disordered along the hexagonal [001] direction.

Allowing for the large standard deviations associated with the occupancy values, the metal atom sites $M(2)$, $M(3)$ are almost empty and the sites $M(4)$, $M(5)$ are almost full. These metal atoms are ordered into alternate octahedral sites, along *c*. Within the basal plane these ordered atoms group together in pairs, or, alternatively, the structure contains ordered pairs of cation vacancies arranged in a specific

TABLE 2. Atomic Parameters for Pseudorutile

	Starting parameters - ideal model				Refined parameters				
Atom	x	y	z	Occupancy	x	y	z	Occupancy	B(Å)^2
M_1	0	0	0	2/3	0	0	0	0.75(15)	
M_2	1/5	0	0	0	0.206(11)	0	0	0.18(6)	
M_3	2/5	0	0	0	0.400(10)	0	0	0.02(6)	
M_4	3/5	0	0	1	0.591(3)	0	0	0.98(8)	1.1(2)
M_5	4/5	0	0	1	0.809(3)	0	0	0.81(7)	
M_6	1/5	2/5	0	2/3	0.184	0.378(3)	0.018(10)	0.67(10)	
M_7	1/5	3/5	0	2/3	0.224(2)	0.605(2)	0.017(22)	0.68(10)	
O_1	2/3	1/3	1/4		0.667(10)	0.333	1/4		
O_2	1/15	2/15	1/4		0.666(12)	0.132	1/4		
O_3	4/15	8/15	1/4		0.260(10)	0.520	1/4		
O_4	1/15	8/15	1/4		0.067(16)	0.533	1/4		1.4(2)
O_5	4/15	2/15	1/4		0.260(20)	0.130	1/4		
O_6	7/15	2/15	1/4		0.067(13)	0.339(9)	0.272(13)		
O_7	1/15	1/3	1/4		0.469(6)	0.129(5)	0.268(15)		

TABLE 3. Calculated and Observed Structure Factors for Pseudorutile

H	K	L	FO	FC	H	K	L	FO	FC	H	K	L	FO	FC	H	K	L	FO	FC
0	5	0	543.5	551.8	2	8	1	*	14.4	5	5	2	156.4	161.5	2	11	3	*	28.6
0	10	0	235.3	243.5	2	9	1	60.0	66.6	5	10	2	214.7	217.6	3	3	3	*	11.2
0	15	0	229.4	222.6	2	10	1	*	44.5	5	15	2	90.3	75.5	3	4	3	*	26.7
5	5	0	762.9	761.1	2	11	1	*	17.4	0	1	3	*	66.8	3	5	3	*	22.0
5	10	0	140.8	113.8	2	12	1	*	33.2	0	2	3	*	13.2	3	6	3	84.0	87.2
10	10	0	140.0	135.2	3	3	1	*	30.0	0	3	3	*	3.2	3	7	3	*	30.6
0	1	1	*	38.1	3	4	1	*	8.0	0	4	3	*	59.0	3	8	3	*	33.4
0	2	1	*	20.6	3	5	1	*	16.7	5	0	3	190.9	221.4	3	9	3	*	13.5
0	3	1	*	32.2	3	6	1	140.5	150.6	0	6	3	*	47.9	3	10	3	*	19.9
0	4	1	*	28.7	3	7	1	*	39.9	0	7	3	*	1.9	3	11	3	72.1	58.4
0	5	1	438.5	415.4	3	8	1	*	25.4	0	8	3	*	5.6	4	4	3	161.3	147.2
0	6	1	*	21.8	3	9	1	*	21.2	0	9	3	*	25.2	4	5	3	*	38.0
0	7	1	*	15.6	3	10	1	*	23.4	0	10	3	100.2	118.9	4	6	3	*	31.2
0	8	1	*	9.3	3	11	1	86.4	55.1	0	11	3	*	25.1	4	7	3	*	31.0
0	9	1	*	22.2	4	4	1	251.8	254.8	0	12	3	*	18.1	4	8	3	*	19.9
0	10	1	170.3	191.9	4	5	1	*	16.6	0	13	3	*	2.9	4	9	3	124.9	138.4
0	11	1	*	5.8	4	6	1	*	38.0	1	1	3	*	83.4	4	10	3	*	9.8
0	12	1	*	29.3	4	7	1	48.0	63.8	1	2	3	*	26.0	5	5	3	*	14.3
0	13	1	*	19.0	4	8	1	*	15.1	1	3	3	182.9	170.0	5	6	3	*	33.6
1	1	1	211.8	208.9	4	9	1	147.6	156.6	1	4	3	*	53.3	5	7	3	*	19.3
1	2	1	*	9.5	5	5	1	*	20.7	1	5	3	*	53.9	5	8	3	*	23.3
1	3	1	199.4	230.7	5	6	1	*	40.4	1	6	3	*	67.2	5	9	3	*	17.4
1	4	1	*	36.8	5	7	1	*	28.6	1	7	3	*	30.2	6	6	3	*	.0
1	5	1	*	42.4	5	8	1	*	28.8	1	8	3	156.6	146.6	6	7	3	*	44.3
1	6	1	*	72.9	5	9	1	*	7.7	1	9	3	*	25.3	6	8	3	121.9	85.7
1	7	1	*	28.8	6	6	1	*	27.1	1	10	3	*	40.6	6	9	3	*	13.7
1	8	1	191.0	184.8	6	7	1	*	16.1	1	11	3	*	29.4	7	7	3	*	24.4
1	9	1	*	17.7	6	8	1	116.0	97.0	1	12	3	*	35.0	7	8	3	*	21.5
1	10	1	*	48.7	6	9	1	*	14.9	1	13	3	94.4	87.5	7	9	3	*	36.8
1	11	1	*	17.5	7	7	1	*	31.7	2	2	3	*	7.9	8	8	3	*	6.1
1	12	1	*	24.7	7	8	1	*	25.2	2	3	3	*	18.7	0	0	4	670.6	659.2
1	13	1	125.9	122.4	7	9	1	*	25.4	2	4	3	69.5	112.0	0	5	4	250.3	285.0
2	2	1	*	18.5	8	8	1	*	15.0	2	5	3	*	34.0	0	10	4	152.0	148.8
2	3	1	*	18.6	8	9	1	*	11.6	2	6	3	*	25.3	0	15	4	159.8	142.1
2	4	1	94.7	130.4	9	9	1	99.3	126.9	2	7	3	*	20.9	5	5	4	260.0	269.7
2	5	1	*	37.8	0	5	2	831.0	824.8	2	8	3	*	11.3	5	10	4	115.7	77.7
2	6	1	*	28.7	0	10	2	385.1	398.9	2	9	3	65.0	64.4					
2	7	1	*	28.3	0	20	2	61.3	44.4	2	10	3	*	31.3					

* Denotes an unobserved reflection

threefold symmetry relationship. This is illustrated more clearly in Figure 4(ii) where the basic structural unit, consisting of three ordered pairs of cation vacancies, is outlined. The ordered metal atoms $M(4)$ and $M(5)$ are octahedrally coordinated to oxygens at distances between 1.92 and 2.11 Å, with average M–O bonds of 1.95 and 2.01 Å respectively. The metal-metal separation across the edge-shared octahedra containing the ordered metals is 3.13 Å. The octahedral anion coordination around the disordered metals $M(6)$ and $M(7)$ is much less regular, with M–O bond lengths in the range 1.84–2.26 Å. This range, although large, may be compared with the M–O range of 1.90-2.25 Å found in another ferric titanate, pseudobrookite (Pauling, 1930).

Figure 4 compares the metal atom arrangements within hexagonal close packed layers for ilmenite, pseudorutile, and triply-twinned rutile. The orientation relationship between the unit cells (Fig. 4) is like that experimentally observed within altered ilmenite grains containing all three phases (Teufer and Temple, 1966). The structural relationship between the three phases, representing successive stages in ilmenite alteration, is apparent from a study of the outlined structural units (Fig. 4, i-iii). The alteration process formally involves a successive growth of cation vacancies within the three symmetry-related [110] chains of octahedra in ilmenite. That the rutile formed is always triply twinned and oriented (Fig. 4, iii) is considered to result from an alteration mechanism involving dissolution followed by epitaxial reprecipitation of TiO_2 in the second stage of the alteration. This is discussed in detail in the following section.

It should be emphasized that the structure obtained for pseudorutile (Fig. 3) results from an idealized treatment of the observed diffraction pattern in which the diffuse diffraction streaks have been treated as discrete reciprocal lattice points defined exactly by the 5× superlattice. The model shown in Figure 3 is thus an averaged representation of the long-range metal-atom ordering, which in fact varies from place to place in the crystal. A more complete understanding of the real situation may be obtained only by a detailed analysis of the geometry of the diffuse scattering. In the absence of a complete

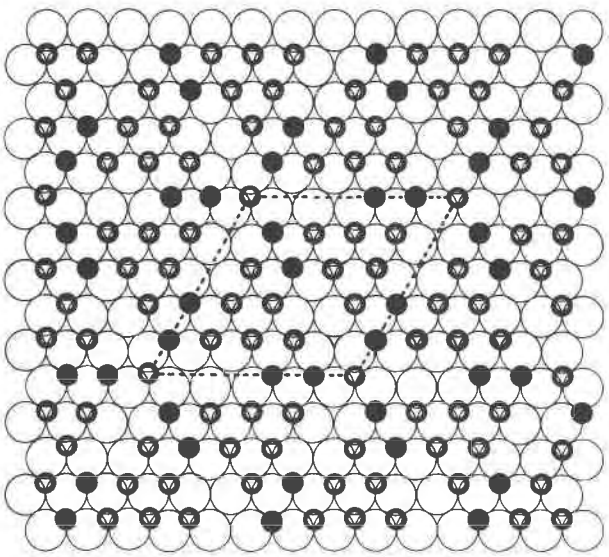

FIG. 3. An (001) section of the structure of pseudorutile showing one hexagonal close-packed oxygen layer (large circles). Fully occupied metal atom sites are shown by the small solid circles, and fractionally occupied metal atom sites are represented by the small open circles. The unit cell outline is dashed.

analysis we can only make the qualitative observation that the diffuse scattering peaks lie in reciprocal (00*l*) planes, indicating a one-dimensional periodic structure parallel to *c*, *i.e.*, a chain structure with a high degree of ordering along the chain but imperfect ordering between chains. In the case of pseudorutile the chains are the [001] rows of alternately filled and empty octahedral sites *M*(2)-*M*(5). Two possibilities exist for ordering between pairs of chains

$$\begin{array}{ll} M\text{-}\square\text{-}M\text{-}\square\text{-}M\text{-}\square & M\text{-}\square\text{-}M\text{-}\square\text{-}M\text{-}\square \\ & \text{or} \qquad\qquad [001]\rightarrow \\ M\text{-}\square\text{-}M\text{-}\square\text{-}M\text{-}\square & \square\text{-}M\text{-}\square\text{-}M\text{-}\square\text{-}M \end{array}$$

where *M* and □ represent filled and empty sites respectively. If the two types of chain are randomly distributed, the corresponding diffraction pattern will exhibit sheets of diffuse intensity perpendicular to [001]. Introduction of correlations between chains results in a modulation of the diffuse intensity within the reciprocal (00*l*) planes. The relatively small extent of diffuse streaking of the metal ordering peaks for pseudorutile (Fig. 2) is consistent with a high degree of correlation between the [001] chains of filled and empty metal atom sites.

The Alteration of Ilmenite

The studies of Teufer and Temple (1966) and the present crystal structure analysis show quite clearly that pseudorutile is a persistent phase with a definite structure and composition. It occurs as a major constituent (Grey and Reid, 1974) of many commercial, altered-ilmenite deposits, and may be considered as a distinct intermediate alteration product of ilmenite in which all the iron has been oxidized to the trivalent state and one-third of it has been leached out, to give the stoichiometry $Fe_2Ti_3O_9$.

In considering why such a composition should be formed as a stable phase, relatively resistant to further alteration, it is worth noting that the pseudorutile stoichiometry corresponds to the maximum removal of iron from the ilmenite structure without concomitant removal of oxygen:

$$3Fe^{2+}TiO_3 \rightarrow Fe_2^{3+}Ti_3O_9 + Fe \qquad \langle 1 \rangle$$

i.e., up to the point of conversion of all Fe^{2+} to Fe^{3+}, metal ion diffusion and oxidation at the crystal surface can account for the change of composition.

Further removal of iron by leaching to eventually produce rutile must involve removal of oxygen also, according to:

$$Fe_2Ti_3O_9 \rightarrow 3TiO_2 + \underbrace{2Fe^{3+} + 3O^{2-}}_{Fe_2O_3} \qquad \langle 2 \rangle$$

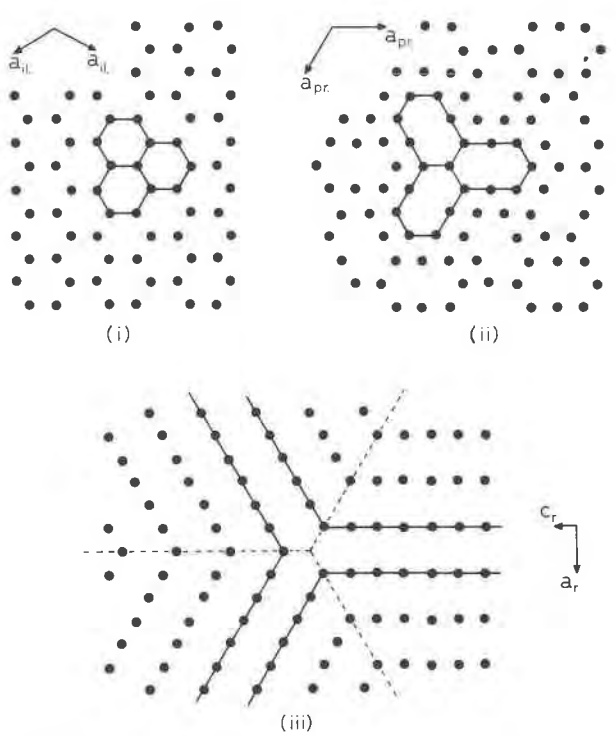

FIG. 4. Metal atom arrangements within hexagonal close-packed anion layers for (i) ilmenite, (ii) pseudorutile, and (iii) triply twinned rutile. The orientations of the unit cells as shown in the diagram are the same as those observed in X-ray diffraction studies on grains of altered ilmenite containing all three phases.

Thus, whereas Reaction ⟨1⟩ may occur topotactically by the diffusion of iron through an essentially unaltered oxygen lattice, the second stage of alteration involves a disruption of the anion lattice as both iron and oxygen are removed.

One might expect that the two alteration reactions, ⟨1⟩ and ⟨2⟩ above, would take place under different environmental conditions, and indeed this has been observed to be the case. Temple (1966) has reported analytical results for a series of drill-hole samples taken from a sand-type deposit of altered ilmenite in Florida. Below the water table level, at about 7 feet and down to about 50 feet, the composition of the altered material was almost constant, with weight percentages of TiO_2, FeO, and Fe_2O_3 of about 66, 2.5, and 30 percent respectively. The analyses correspond quite closely to those for pseudorutile (*cf* Indonesian pseudorutile, Table 1). Thus, the material taken from below the water table represents the first stage in the alteration of ilmenite (Reaction 1). Above the water table the composition of the altered ilmenite changed markedly, with TiO_2 analyses up to 83 percent and Fe_2O_3 analyses below 15 percent; only in the top few feet of the deposit does the second alteration stage (Reaction ⟨2⟩ above) proceed to any extent in the Florida deposit. Similar results were obtained from studies on drill-hole samples from other localities.

Models for the Alteration Mechanism

A feasible explanation for these observations is that in the zone of saturation the oxidation and leaching proceeds via an electrochemical corrosion process, whereas in the zone of oxidation the material is leached via a dissolution and reprecipitation process. Considering these two processes in turn, the electrochemical corrosion model has recently been applied to the case of mineral oxidation to explain the oxidation of sulfide minerals in ground water situations (Sato, 1960a,b; Nickel, Ross, and Thornber, 1974). Natural ilmenites containing some ferric iron (*e.g.*, as Fe_2O_3–$FeTiO_3$ solid solutions) are quite good conductors, and in suitable ground water situations might also be expected to oxidize by this process. Possible half-cell reactions may be written

$$\text{anodic:}\quad Fe^{2+} \rightarrow Fe^{3+} + e$$
$$\text{cathodic:}\quad \tfrac{1}{2}O_2 + \tfrac{1}{2}H_2O + e \rightarrow 1/3\cdot(OH)_3^{3-}$$

In situ anodic oxidation of ferrous ions produces electrons which can move through the conducting solid to the surface (or to a crack or fault in the grain) and take part in cathodic reduction of oxygen in the ground water. The above half-cell reactions show that *complete* oxidation of the ferrous iron in ilmenite to ferric iron releases one electron; this will produce just enough hydroxyl ion (or some other negatively charged anion) at the cathode to remove *one-third* of the ferric ions produced. If we assume that the oxygen content remains constant, then the end product of electrochemical alteration of ilmenite is $Fe^{3+}{}_{2/3}\,TiO_3 \equiv Fe_2Ti_3O_9$, the pseudorutile composition. Thus, the electrochemical corrosion model is consistent with the pseudorutile composition being a stable alteration product of ilmenite in which all the iron is in the ferric state. Although the model does not require the addition or removal of oxygen from the anion lattice, the change from ilmenite to pseudorutile results in a volume reduction of about 6 percent which would produce considerable elastic stress in the oxygen lattice at the coherent interface between segments of ilmenite and its alteration product, pseudorutile. This would result in the development of considerable microcracking and poring. Consistent with this, an electron microscope study of the surface of pseudorutile shows it to have a very fine granularity, about 30 Å in diameter (Temple, 1966).

In contrast, electron microscope images of more highly altered ilmenites, approaching TiO_2 in composition, show a much coarser microstructure with crystallites up to 500 Å in diameter (Temple, 1966). This suggests that alteration beyond the pseudorutile composition occurs via a leaching and reprecipitation process whereby both iron oxide and titanium oxide go into solution and then titanium oxide reprecipitates on the seed material. Such a mechanism could change the microscopic features such as granularity or crystallite size, while maintaining the overall macroscopic morphology. *Epitactic* reprecipitation of titanium oxide on the original material would also be consistent with the observation of a triply twinned alteration product; *i.e.*, the rutile is adjusting to the hexagonal symmetry of an undissolved pseudorutile crystallite. We envisage this alteration mechanism to occur in the top few feet of the deposit where the upper soil layer decomposes to form active organic acids and carbonic acids (Dyadchenko and Khatuntseva, 1960) capable of dissolving the pseudorutile. In this upper region of maximum temperature fluctuation, fluctuating water level, and ready access of atmospheric oxygen, mechanical weathering must also assist in the chemical weathering. Finally, the role of bacteria and metal-specific microorganisms may also contribute to the dissolution process.

Acknowledgments

The authors wish to thank Drs Brian Gatehouse and Barry Miskin for kindly making available their crystallographic computing programs and their precession camera. We would also like to thank Dr K. J. Henley of Amdel for the samples of pseudorutile, and gratefully acknowledge the analytical work of Mrs C. Li and Mr G. Dark in the CSIRO laboratories.

References

Bailey, S. W., E. N. Cameron, H. R. Spedden, and R. J. Weege (1956) The alteration of ilmenite in beach sands. *Econ. Geol.* **51,** 263–279.

Busing, W. R., K. O. Martin, and H. A. Levy (1962) Orfls, a Fortran crystallographic least-squares program. *U.S. Nat. Tech. Inform. Serv.* Ornl-tm-**305,** Oak Ridge National Laboratory, Oak Ridge, Tennessee.

Bykov, A. D. (1964) Proarizonite as a secondary mineral due to supergene alteration of ilmenite. *Dokl. Akad. Nauk SSSR,* **156,** 567–570.

Dyadchenko, M. G., and A. Ya. Khatuntseva (1960) Mineralogy and petrology of the weathering process in ilmenite. *Dokl. Akad. Nauk SSSR,* **132,** 435–438.

Ernst, T. (1943) Fusion equilibria in the system Fe_2O_3–FeO–TiO_2 and notes on the minerals arizonite and pseudobrookite. *Z. Angew. Mineral.* **4,** 394–409.

Grey, I. E., and A. F. Reid (1974) Reaction sequences in the reduction of ilmenite: 3-Reduction in a commercial rotary kiln; an X-ray diffraction study. *Inst. Mining Met. Trans., Sect. C,* **83,** 39–46.

Koch, F., and J. B. Cohen (1969) The defect structure of $Fe_{1-x}O$. *Acta Crystallogr., Sect. B,* **25,** 275–287.

Larrett, M. J. W., and W. G. Spencer (1971) Contributions to Australasian mineralogy: 3. 'Pseudorutile' from South Neptune Island, South Australia. *Amdel Bull.* **12,** 74–80.

Lynd, L. E., H. Sigurdson, C. H. North, and W. W. Anderson (1954) Characteristics of titaniferous concentrates. *Trans. AIME 199, Tech. Publ.* **3815-H** (in *Mining Eng.* **6,** 817–24).

Miller, R. (1945) The heavy minerals of Florida beach and sand dunes. *Am. Mineral.* **30,** 65–75.

Nickel, E. H., J. R. Ross, and M. R. Thornber (1974) The supergene alteration of pyrrhotite-pentlandite ore at Kambalda, Western Australia. *Econ. Geol.* **69,** 93–108.

Overholt, J. L., G. Vaux, and J. L. Rodda (1950) The nature of "arizonite." *Am. Mineral.* **35,** 117–119.

Palmer, C. (1909) Arizonite, ferric metatitanate. *Am. J. Sci.* **28,** 353–356.

Pauling, L. (1930) The crystal structure of pseudobrookite. *Z. Kristallogr., Kristallgeom. Kristallphys. Kristallchem.* **73,** 93–112.

Sato, M. (1960a) Oxidation of sulphide ore bodies. I. Geochemical environments in terms of Eh and pH. *Econ. Geol.* **55,** 228–261.

——— (1960b) Oxidation of sulphide ore bodies. II. Oxidation mechanisms of sulphide minerals at 25°C. *Econ. Geol.* **55,** 1202–1231.

Temple, A. K. (1966) Alteration of ilmenite. *Econ. Geol.* **61,** 695–714.

Teufer, G., and A. K. Temple (1966) Pseudorutile—a new mineral intermediate between ilmenite and rutile in the natural alteration of ilmenite. *Nature (London),* **211,** 179–181.

Manuscript received, November 18, 1974; accepted for publication, March 21, 1975.